
PERGAMON

Journal of the Mechanics and Physics of Solids
48 (2000) 461–498

JOURNAL OF THE
MECHANICS AND
PHYSICS OF SOLIDS

www.elsevier.com/locate/jmps

Multiphase composites with extremal bulk modulus

Leonid V. Gibiansky[a, 1], Ole Sigmund[b,*]

[a]*49 Flints Grove Drive, North Potomac, MD 20878, USA*
[b]*Department of Solid Mechanics, Technical University of Denmark, Building 404, DK-2800, Lyngby, Denmark*

Received 18 January 1999; received in revised form 28 May 1999

Abstract

This paper is devoted to the analytical and numerical study of isotropic elastic composites made of three or more isotropic phases. The ranges of their effective bulk and shear moduli are restricted by the Hashin–Shtrikman–Walpole (HSW) bounds. For two-phase composites, these bounds are attainable, that is, there exist composites with extreme bulk and shear moduli. For multiphase composites, they may or may not be attainable depending on phase moduli and volume fractions. Sufficient conditions of attainability of the bounds and various previously known and new types of optimal composites are described. Most of our new results are related to the two-dimensional problem. A numerical topology optimization procedure that solves the inverse homogenization problem is adopted and used to look for two-dimensional three-phase composites with a maximal effective bulk modulus. For the combination of parameters where the HSW bound is known to be attainable, new microstructures are found numerically that possess bulk moduli close to the bound. Moreover, new types of microstructures with bulk moduli close to the bound are found numerically for the situations where the aforementioned attainability conditions are not met. Based on the numerical results, several new types of structures that possess extremal bulk modulus are suggested and studied analytically. The bulk moduli of the new structures are either equal to the HSW bound or higher than the bulk modulus of any other known composite with the same phase moduli and volume fractions. It is proved that the HSW bound is attainable in a much wider range than it was

* Corresponding author.
E-mail address: sigmund@fam.dtu.dk (O. Sigmund).

[1] The paper was written while L. Gibiansky was visiting the Department of Solid Mechanics, Technical University of Denmark

PII: S0022-5096(99)00043-5

previously believed. Results are readily applied to two-dimensional three-phase isotropic conducting composites with extremal conductivity. They can also be used to study transversely isotropic three-dimensional three-phase composites with cylindrical inclusions of arbitrary cross-sections (plane strain problem) or transversely isotropic thin plates (plane stress or bending of plates problems).

Keywords: Homogenization; A. Microstructures; B. Constitutive behaviour; C. Optimization; Numerical algorithms

1. Introduction

The paper is devoted to the long-standing problem of bounds on effective properties of elastic composites comprised of isotropic phases. We aim to achieve three goals.

In Section 2, we investigate sufficient conditions for the attainability of the Hashin and Shtrikman (1963) and Walpole (1966) bounds. These are the simple conditions on phase properties and volume fractions that guarantee existence of multiphase composites with a bulk or shear modulus exactly equal to the bounds. For the bulk modulus problem, these attainability conditions were found by Milton (1981). Here we formulate analogous conditions for the shear modulus problem. When these conditions are met, we demonstrate several microstructures that achieve the bounds.

The goal in Section 3 is to search for two-dimensional three-phase composites with a maximal bulk modulus by using a numerically based topology optimization method. We start with the situation where the bound is known to be optimal. The goal is to check the reliability of the inverse homogenization procedure (Sigmund, 1994a, b, 1995, 1999a, b; Sigmund and Torquato, 1996, 1997) by solving a problem with known answer, that is, with known optimal bound. The result of the check is more than satisfactory. The procedure not only found a microstructure with an extremal bulk modulus but this microstructure was of a new (although similar to the known) type. Then we used the same procedure to explore parameter regions where the optimal structures were not known. The parameters of the problem were slowly changed and the evolution of the optimal design was studied. New structures were found for the range of parameters where the attainability conditions for the Hashin–Shtrikman–Walpole (HSW) bulk modulus upper bound are not met. The bulk modulus of each of these new structures is higher than the bulk modulus of any previously known composite with the same phase moduli and volume fractions. The HSW bulk modulus bounds apply not only to isotropic composites, but also to composites with square symmetry (in two dimensions) or cubic symmetry (in three dimensions) of the elastic tensor. In our numerical and analytical study of two-dimensional structures we require only square symmetry of the effective tensor. However, given material with square symmetry one can easily make an isotropic composite with the same value of

effective bulk modulus. Alternatively, the numerical procedure can solve the problem with some extra computational effort.

Section 4 is devoted to the theoretical study of two-dimensional three-phase composites with a maximal bulk modulus. We found several new types of three-phase structures based on a new class of extremal two-phase composites proposed recently by one of the authors (Sigmund, 1999b) and on the result of our numerical experiments in Section 3. The microstructures of two of the new types have an effective bulk moduli exactly equal to the HSW bulk modulus bounds in a range of parameters where more traditional approaches have failed to deliver optimal composites. When the volume fraction of the stiff phase is low, we found another new type of composite which has an effective bulk modulus that is smaller than the bound but larger than the bulk modulus of any previously known composite with the same phase moduli and volume fractions.

In Section 5 we summarize, discuss, and generalize the results of the paper. In particular, two-dimensional three phase composites with extremal conductivity are discussed. We show that the bulk modulus results for the phases with zero Poisson's ratio are readily applied to conductivity. Thus, two new types of conducting composites are found. The microstructures of one of the new types have effective conductivity exactly equal to the Hashin–Shtrikman (HS) bound in the range of the parameters where previously known composites were not optimal. Outside of the parameter range where the HS bound is attainable, we found another new type of composite which has effective conductivity that is not equal to the bound but closer to the bound than the conductivity of any previously known composite with the same phase moduli and volume fractions.

The obtained results can be applied to the effective moduli of a transversely isotropic three-dimensional composite with cylindrical inclusions of an arbitrary cross-section. They can also be applied to the effective plane stress or bending moduli of thin plates with the microstructure independent of the coordinate perpendicular to the plate.

2. Known bounds on effective moduli and optimal microstructures

2.1. Hashin–Shtrikman–Walpole bounds

We deal with the linear elasticity problem. The stiffness of an isotropic elastic material can be described by two moduli, that is, the bulk modulus κ and the shear modulus μ. We consider a composite made of N elastic phases, with bulk moduli κ_i and shear moduli μ_i, taken in the prescribed volume fractions f_i, $i = 1, \ldots, N$. An isotropic composite is characterized by its effective bulk modulus κ_* and its effective shear modulus μ_*. For accounts of homogenization theory, see for example Bensoussan et al. (1978), Sanchez-Palencia (1980), Jikov et al. (1994).

Hashin and Shtrikman (1963) suggested variational principles which allowed them to find tight bounds on the effective elastic moduli of an isotropic composite made from isotropic phases. Hashin (1965) applied the same method to obtain

bounds for the transversely isotropic composites with cylindrical inclusions. The phases were supposed to be 'well-ordered' so that the phase with the largest (smallest) bulk modulus also had the largest (smallest) shear modulus. Walpole (1966) developed a similar variational method and derived bounds that did not require any phase ordering. For the well-ordered phases, the Walpole bounds are equivalent to the HS ones.

The HSW bounds have the form

$$\kappa_{\mathrm{L}} \leq \kappa_* \leq \kappa_{\mathrm{U}}, \quad \mu_{\mathrm{L}} \leq \mu_* \leq \mu_{\mathrm{U}}, \tag{1}$$

where

$$\kappa_{\mathrm{L}} \left[\sum_{i=1}^{N} \frac{f_i}{\kappa_i + y_\kappa^{\mathrm{L}}} \right]^{-1} - y_\kappa^{\mathrm{L}}, \quad y_\kappa^{\mathrm{L}} = \frac{2(d-1)}{d} \mu_{\min}, \tag{2}$$

$$\kappa_{\mathrm{U}} \left[\sum_{i=1}^{N} \frac{f_i}{\kappa_i + y_\kappa^{\mathrm{U}}} \right]^{-1} - y_\kappa^{\mathrm{U}}, \quad y_\kappa^{\mathrm{U}} = \frac{2(d-1)}{d} \mu_{\max}, \tag{3}$$

$$\mu_{\mathrm{L}} = \left[\sum_{i=1}^{N} \frac{f_i}{\mu_i + y_\mu^{\mathrm{L}}} \right]^{-1} - y_\mu^{\mathrm{L}},$$

$$y_\mu^{\mathrm{L}} = \frac{\kappa_{\min}\, \mu_{\min}}{\kappa_{\min} + 2\mu_{\min}} \ (d=2), \quad y_\mu^{\mathrm{L}} = \frac{\mu_{\min}\, (9\kappa_{\min} + 8\mu_{\min})}{6\kappa_{\min} + 12\mu_{\min}} \ (d=3), \tag{4}$$

$$\mu_{\mathrm{U}} = \left[\sum_{i=1}^{N} \frac{f_i}{\mu_i + y_\mu^{\mathrm{U}}} \right]^{-1} - y_\mu^{\mathrm{U}},$$

$$y_\mu^{\mathrm{U}} = \frac{\kappa_{\max}\, \mu_{\max}}{\kappa_{\max} + 2\mu_{\max}} \ (d=2), \quad y_\mu^{\mathrm{U}} = \frac{\mu_{\max}\, (9\kappa_{\max} + 8\mu_{\max})}{6\kappa_{\max} + 12\mu_{\max}} \ (d=3). \tag{5}$$

Here, $\kappa_{\min}$ ($\kappa_{\max}$) and $\mu_{\min}$ ($\mu_{\max}$) are the minimal (maximal) values of the phase bulk and shear moduli, respectively, and $d = 2$ or $d = 3$ is the spatial dimension.

It is known that the two-phase HS bounds (1) ($d = 2$) are optimal in the sense that there exist special microstructures (Hashin and Shtrikman, 1963) with an effective bulk moduli equal to κ_{L} and κ_{U}. It is also known that for more than two phases these bounds cannot be optimal in the whole range of parameters. Indeed, consider the upper bound κ_{U} for the situation where the volume fraction of the stiff phase (with large but finite shear modulus $\mu = \mu_{\max}$) vanishes. One can see that the bound still depends on the shear modulus of the phase with zero volume fraction. However, effective moduli of any composite cannot depend on the moduli of the phase with finite moduli and zero volume fraction.

2.2. Optimal two-phase composites

For two well-ordered phases such that

$$(\kappa_1 - \kappa_2)(\mu_1 - \mu_2) \geq 0, \tag{6}$$

Lurie and Cherkaev (1984), Norris (1985), Milton (1986), and Francfort and Murat (1986) found composites with effective moduli

$$\kappa_* = \kappa_{\mathrm{L}}, \quad \mu_* = \mu_{\mathrm{L}}, \tag{7}$$

and composites with effective moduli

$$\kappa_* = \kappa_{\mathrm{U}}, \quad \mu_* = \mu_{\mathrm{U}}, \tag{8}$$

that are equal to the HSW bounds. The optimal two-phase microstructures will be used to construct optimal multiphase composites in this paper. For these reasons, we briefly describe them here.

2.2.1. Coated spheres composite (Hashin and Shtrikman, 1963)

This is the first microstructure that was shown to exhibit a bulk modulus equal to the bound. It consists of coated spheres (circles in two dimensions) made of a core of phase i and external coating of phase j, that fill the whole space. The bulk modulus of this composite is given by the solution to

$$\frac{1}{\kappa_* + y_\kappa^j} = \frac{f_i}{\kappa_i + y_\kappa^j} + \frac{f_j}{\kappa_j + y_\kappa^j}, \quad y_\kappa^j = \frac{2(d-1)}{d}\mu_j. \tag{9}$$

The shear modulus of such a composite is equal to the HSW bound only in the limit of infinitesimal volume fraction of phase j. This fact is used in the following type of optimal composite.

2.2.2. Differential process

A differential process that allows one to obtain structures with extremal bulk and shear moduli was suggested independently by Lurie and Cherkaev (1984) and Norris (1985). One starts with a core of phase i. Then one sequentially adds infinitesimal portions of phase j. The microstructure of the composite on each differential step is assumed to be described by the coated spheres construction. This is continued until the available amount of phase j is used. The effective bulk modulus of the resulting composite is given by (9), and the effective shear modulus is given by

$$\begin{gathered} \frac{1}{\mu_* + y_\mu^i} = \frac{f_i}{\mu_i + y_\mu^j} + \frac{f_j}{\mu_j + y_\mu^j}, \\ y_\mu^j = \frac{\kappa_j \mu_j}{\kappa_j + 2\mu_j} \ (d=2), \quad y_\mu^j = \frac{\mu_j(9\kappa_j + 8\mu_j)}{6\kappa_j + 12\mu_j} \ (d=3). \end{gathered} \tag{10}$$

2.2.3. Matrix laminate composite

Milton (1986) and Francfort and Murat (1986) have shown that matrix laminate composites of high rank have effective bulk and shear moduli given by (9) and (10), respectively, where i is the inclusion phase, and j is the matrix phase.

2.2.4. Vigdergauz (1989) structures

Vigdergauz found two-dimensional two-phase square symmetric (Vigdergauz, 1989; Grabovsky and Kohn, 1995) and isotropic (Vigdergauz, 1999) microstructures with extremal bulk moduli. They consist of periodic arrays of phase i inclusions in phase j matrix. The shape of the inclusions is described analytically in terms of special functions. The effective bulk moduli of these composites are given by (9); the effective shear moduli are not extreme. Three-dimensional versions of these structures have been found only numerically (Vigdergauz, 1994; Sigmund, 1999a).

2.2.5. Structures by Sigmund (1999b)

Recently one of the authors suggested a new type of square symmetric (in two dimensions) or cubic symmetric (in three-dimensional space) and isotropic structures with extremal bulk modulus (Sigmund, 1999b). A two-dimensional square symmetric example of these structures is shown in Fig. 1. It consists of a core of phase i, corner blocks of phase j, and laminates of phases i and j taken in equal proportions $\rho_1 = \rho_2 = 1/2$, with the lamination parallel to phase i and normal to phase j. It is assumed that the length-scale of the lamination is much smaller than the size of the periodic cell so that the laminate composite can be treated as homogeneous anisotropic material illustrated in Fig. 1 by the strips of different

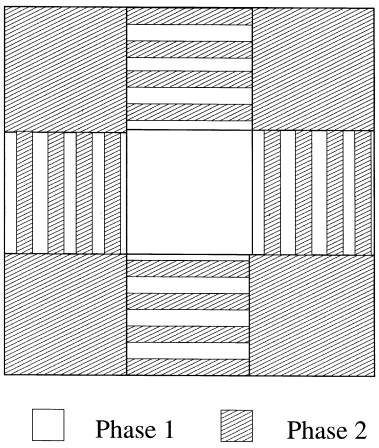

Fig. 1. Sigmund (1999b) two-phase square symmetric microstructure with effective bulk modulus equal to the HSW bound. Volume fractions of phases 1 and 2 in the lamination regions (schematically shown by the alternating strips of phases 1 and 2) are equal.

phases. Any isotropic or square symmetric microstructure that satisfies aforementioned simple geometrical requirements has the effective bulk modulus given by (9). Similar three-dimensional structures can also be found (see Sigmund, 1999b for details). The effective shear moduli of isotropic composites of the described type can vary in an interval almost equal to the theoretical limits for the composite with extremal bulk modulus. However, their shear moduli are not shown to be exactly equal to the HSW bounds.

All the considered materials have one common feature: one phase forms inclusions in a matrix of the other phase. If the structure is subject to hydrostatic external field, stresses and strains in the inclusions are constant, which is necessary for the optimality of the effective bulk modulus. Similarly, if the structure is subject to a deviatoric (pure shear) external field, stresses and strains in the inclusions are constant for the differential scheme composite and in the matrix laminate composite. This is also necessary for the optimality of the effective shear modulus for a composite of two well-ordered phases.

2.3. Multiphase composites with extreme bulk modulus

Milton (1981) has shown that the HSW bulk modulus bounds for multiphase composites are attainable subject to some restrictions on phase moduli and volume fractions. Here we follow his description. Specifically, we number phases so that

$$\kappa_1 \leq \kappa_2 \leq \kappa_3 \leq \cdots \leq \kappa_N. \tag{11}$$

Then the HSW lower bound (2) is attainable if

$$\mu_1 = \mu_{\min}, \quad \kappa_L \leq \kappa_2, \tag{12}$$

or if

$$\mu_N = \mu_{\min}, \quad \kappa_L \geq \kappa_{N-1}. \tag{13}$$

Similarly, the HSW upper bound (3) is attainable if

$$\mu_1 = \mu_{\max}, \quad \kappa_U \leq \kappa_2, \tag{14}$$

or if

$$\mu_N = \mu_{\max}, \quad \kappa_U \geq \kappa_{N-1}. \tag{15}$$

We assume that (15) holds and briefly describe structures with maximal bulk modulus in the following. The other case (14) and the microstructures that attain the lower bound can be described almost literally following this derivation. The procedure is based on availability of the two-phase composite with an extremal bulk modulus. Milton (1981) used coated spheres but one can use any other type of optimal composite described in the previous section.

One starts by preparing optimal two-phase composites of $(N-1)$ different

types. All these composites have matrix of phase N but different inclusion phases. The whole available amount of phase N is distributed between these $(N-1)$ composite types according to the solution of the system of equations

$$\begin{aligned} &\frac{f_i/(f_i+\delta_i f_N)}{\kappa_i+y_\kappa^N}+\frac{\delta_i f_N/(f_i+\delta_i f_N)}{\kappa_N+y_\kappa^N}=\frac{1}{\kappa_{\mathrm{U}}+y_\kappa^N}, \quad i=1,\ \ldots,\ N-1,\\ &\sum_{i=1}^{N-1}\delta_i=1, \end{aligned} \tag{16}$$

where y_κ^N is defined as in (3). Thus, they all have the same bulk modulus κ_{U} equal to the HSW bound. Conditions (15) guarantee that parameters δ_i belong to the intervals $\delta_i \in [0,\ 1]$. After having prepared these composites, one mixes them together retaining their common bulk modulus κ_{U}. The process is schematically illustrated by Fig. 2. The effective bulk modulus of the resulting composite is exactly equal to the upper bound κ_{U}.

An alternative construction schematically illustrated by Fig. 3 was proposed by Lurie and Cherkaev (1984) who studied multiphase conducting composites. They suggested to start by preparing an optimal composite of the whole available amount of phase 1 (with the smallest bulk modulus) surrounded by a matrix of phase N (with the largest value of y_κ^N). The amount γf_N of phase N that is used at this stage is given by a solution γ_* of the equation

$$\frac{1}{\kappa_2+y_\kappa^N}=\frac{f_1/(f_1+\gamma f_N)}{\kappa_1+y_\kappa^N}+\frac{\gamma f_N/(f_1+\gamma f_N)}{\kappa_N+y_\kappa^N}. \tag{17}$$

The condition (17) ensures that the resulting composite has effective bulk modulus exactly equal to κ_2. At the next stage of the process this composite is mixed with

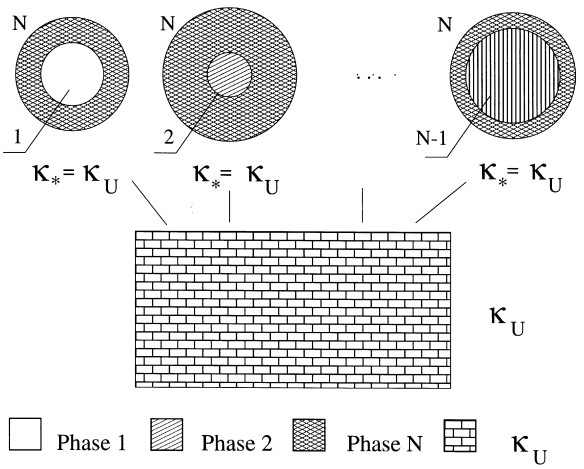

Fig. 2. Milton (1981) scheme to build a multiphase composite with maximal bulk modulus.

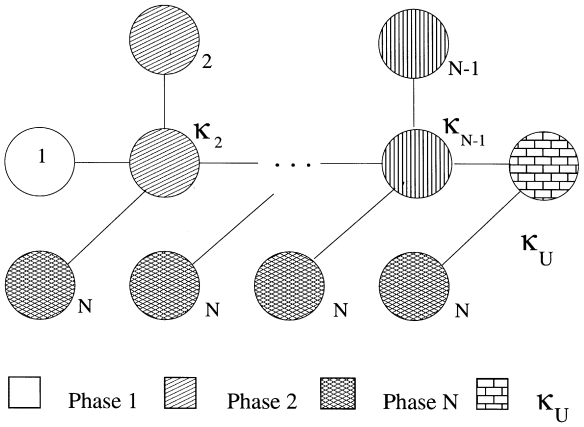

Fig. 3. Lurie and Cherkaev (1984) scheme to build a multiphase composite with maximal bulk modulus.

the whole available amount of phase 2, still having the effective bulk modulus exactly equal to κ_2. Now the phase with the smallest bulk modulus has been 'eliminated' and one is left with $(N-1)$ phases with new volume fractions of phases 2 and N. One continues the process by mixing together the composite obtained at stage k with some amount of phase N sufficient to make the effective bulk modulus equal to the smallest of the bulk moduli of the remaining phases. Then one adds the whole amount of the weakest phase, and continues in this fashion until all phases have been used. At the last stage of the process the remaining amount of phase N is added. The resulting composite has bulk modulus exactly equal to the HSW bound.

Such a process is feasible provided one has a sufficient amount of phase N. If (at any stage of the process) the required amount of phase N is larger than the available amount f_N, the described procedure would not work. The limiting case is when the HSW bound is exactly equal to κ_{N-1}. Thus, the attainability condition, that is, the condition for phase moduli and volume fractions that allows one to build a composite with bulk modulus exactly equal to the upper bound (3), is given by (15).

All the considered materials have one feature in common: phase N forms the matrix and all the other phases form inclusions in this matrix. If the structure is subject to a hydrostatic average field, stress and strain fields in the inclusions are constant (although different in each phase). In fact, the HSW bounds were derived by using (in the Hashin and Shtrikman, 1963 variational principles) trial fields which were constant in all phases except phase N. For the bound to be attainable, the trial field used in the derivation of the bounds should coincide with the actual field in the composite. Therefore, the constantness of the fields in all phases except phase N, in a structure subjected to hydrostatic load, is a necessary condition for

the effective bulk modulus to be equal to the HSW bound. We will refer to this requirement as field optimality conditions.

2.4. Multiphase composites with an extreme shear modulus

It is easy to generalize the process described above to study multiphase composites with maximal shear modulus. We number the phases according to their shear moduli, that is,

$$\mu_1 \le \mu_2 \le \mu_3 \le \cdots \le \mu_N. \tag{18}$$

Then the HSW shear modulus lower bound (4) is attainable if

$$\kappa_1 = \kappa_{\min}, \quad \mu_L \le \mu_2, \tag{19}$$

and the HSW upper bound (5) is attainable if

$$\kappa_N = \kappa_{\max}, \quad \mu_U \ge \mu_{N-1}. \tag{20}$$

The process of building multiphase composites with extremal effective bulk moduli was based on the availability of optimal two-phase composites that correspond to the HSW bulk modulus bound. For the shear modulus problem, our choice is more limited, since only the differential scheme and the matrix laminate composites are known to have extremal shear modulus equal to the HSW bound. Therefore, only the constructions based on these schemes will work for the multiphase design. Apart from that, there is a one-to-one correspondence between the extremal bulk and shear extremal modulus procedures provided we replace κ and y_κ by μ and y_μ in all the formulas.

Unlike the two-phase problem, there is no known multiphase composite that simultaneously achieves both bulk and shear HSW bounds. Indeed, the distribution of phases between the different types of composite in the Milton (1981) procedure, or the rule of adding phases in the Lurie and Cherkaev (1984) procedure depend on phase bulk moduli for the bulk modulus optimization, and on phase shear moduli for the shear modulus optimization. Thus, the microstructure of the composite with optimal effective bulk modulus differs from the one with optimal effective shear modulus.

3. Numerical design of extreme materials

In this section the numerically based material design or 'inverse homogenization' procedure is briefly reviewed, and then used for the two-dimensional three-phase bulk modulus optimization problem.

3.1. Inverse homogenization procedure

The inverse homogenization procedure applied here, solves the following

problem: for given volume fractions find the microstructural topology which extremizes the bulk modulus for a three-phase composite. The procedure is based on the homogenization theory (see Bensoussan et al., 1978; Sanchez-Palencia, 1980; Jikov et al., 1994) and the topology optimization method (see Bendsøe and Kikuchi, 1988 or Bendsøe, 1995 for an overview) and consists of solving a sequence of finite element problems followed by design changes. The material microstructure is assumed to be periodic and fully described by its smallest repetitive unit, the base cell. The base-cell is discretized by several thousand finite elements. The effective properties are found using a numerical homogenization procedure using finite element analysis to find the local fields and applying the appropriate periodic boundary conditions (Bourgat, 1977; Guedes and Kikuchi, 1991).

The material topology optimization procedure (Sigmund, 1994a, b, 1995, 1999a, b; Sigmund and Torquato, 1996, 1997), solves the problem of finding the pointwise distribution of isotropic material phases in the design domain Ω (the base cell) that extremizes the effective bulk modulus, with prescribed volume fractions of phases 1 to 3

$$\begin{aligned} &\max_{\chi_1(x),\ \chi_2(x),\ \chi_3(x)} : \quad \kappa_*(\chi_1, \chi_2, \chi_3), \\ &\text{s.t.:} \quad \langle \chi_1 \rangle = f_1, \quad \langle \chi_2 \rangle = f_2, \quad \langle \chi_3 \rangle = f_3, \\ &\text{s.t.:} \quad \text{material symmetry requirements}, \\ &\text{s.t.:} \quad \text{frequency of material variation}, \end{aligned} \tag{21}$$

where κ_* is the effective bulk modulus of the composite, $\chi_i(x)$ is the indicator function of phase i at a point x, that is,

$$\chi_i(x) = \begin{cases} 1 & \text{if } x \text{ in phase } i, \\ 0 & \text{otherwise.} \end{cases} \qquad \chi_1(x) + \chi_2(x) + \chi_3(x) = 1; \tag{22}$$

angular brackets denote averaging over the periodic cell, f_i is the phase i volume fraction. Material symmetry requirements mean that we will look for a composite with an isotropic or square symmetric effective stiffness tensor, and the frequency of the material variation is limited to assure existence, avoidance of checker-board-type instabilities and removal of mesh-dependencies in the design. We will discuss them later.

The material properties at a point x are specified by

$$C_{ijkl}(x) = \chi_1(x) C^{(1)}_{ijkl} + \chi_2(x) C^{(2)}_{ijkl} + \chi_3(x) C^{(3)}_{ijkl}, \tag{23}$$

where $C^{(i)}_{ijkl}$ is the constitutive tensor of isotropic material phase i

$$C^{(i)}_{ijkl} = \kappa_i \delta_{ij}\delta_{kl} + \mu_i\left(\delta_{ik}\delta_{jl} + \delta_{il}\delta_{jk} - \frac{2}{d}\delta_{ij}\delta_{kl}\right), \tag{24}$$

δ_{ij} is Kronecker's delta, and d is the dimension.

It is convenient for the optimization procedure to present dependence of the local stiffness on the position x in the form

$$C_{ijkl}(x) = \chi_{23}(x)\left\{[1-\chi_3(x)]C^{(2)}_{ijkl} + \chi_3(x)C^{(3)}_{ijkl}\right\} + [1-\chi_{23}(x)]C^{(1)}_{ijkl}, \tag{25}$$

where $\chi_{23} = \chi_2(x) + \chi_3(x)$ is the indicator function of phases 2 and 3 combined. The advantage of such a representation is that the design is now defined by the values of two arbitrary indicator functions $\chi_3(x)$ and $\chi_{23}(x)$, whereas in the representation (23) one should take the condition $\chi_1 + \chi_2 + \chi_3 = 1$ into account.

In practice, the base cell is discretized by a finite number of elements and the material type of each element is then the design variable. For computational reasons, the integer-type optimization problem is converted into a continuous problem by allowing mixtures of materials in each element during the optimization process. This is done by introducing, for each element, two continuous density variables $\rho_{23}(x)$ and $\rho_3(x)$ both defined on the interval [0; 1]. In our numerical examples, phase 1 material is fixed to be void. Using these assumptions, the constitutive tensor for an element is then defined as

$$C_{ijkl}(\rho_{23}, \rho_3) = (\rho_{23})^p\left\{[1-(\rho_3)^q]C^{(2)}_{ijkl} + (\rho_3)^q C^{(3)}_{ijkl}\right\}, \tag{26}$$

where $p > 1$ and $q > 1$ are penalization factors used to prevent intermediate values of the density variables ρ_{23} and ρ_3 in the final design. By choosing p and q low (we used $p = q = 3$) in the beginning of the design process, intermediate densities and mixtures of phases are allowed. This prevents the algorithm from getting stuck in local minima. During the design process, the penalization factors are gradually increased. This makes the use of mixtures or intermediate densities 'un-economical' and enforces the design variables to take their extreme values. Volume fraction restrictions are expressed in terms of the functions ρ_{23} and ρ_3 as

$$\langle 1-\rho_{23}\rangle = f_1, \quad \langle \rho_{23}(1-\rho_3)\rangle = f_2, \quad \langle \rho_{23}\rho_3\rangle = f_3. \tag{27}$$

Orthotropy or isotropy of the resulting microstructures is ensured by specifying at least one line of symmetry and making (numerically) sure that the conditions $C^{(*)}_{1111} - C^{(*)}_{2222} = 0$ and $C^{(*)}_{1111} + C^{(*)}_{2222} - 2(C^{(*)}_{1122} + 2C^{(*)}_{1212}) = 0$ are satisfied for the resulting effective stiffness tensor $C^{(*)}_{ijkl}$.

The computational procedure has a built-in low-pass filtering scheme that allows the user to control the minimal length-scale in the composite microstructure (Sigmund, 1994b, 1997; Sigmund and Petersson, 1998). Varying the filter parameter makes it possible to control the result to a certain extent. It was demonstrated for two-phase problems (Sigmund, 1999b) that a low value of the low-pass filter parameter results in Vigdergauz-like one-length-scale

microstructure, whereas a high value can also result in microstructures with laminations.

Typically, a full optimization process requires a thousand iterations and some interactions by the operator. Depending on the discretization the time used to optimize a microstructure may take from one to several hours on a fast workstation.

The solutions obtained from the topology optimization procedure are generally non-unique. Depending on starting guess, shape of base-cell, filter parameters and other parameters, different topologies may occur. For example, the same topology can occur in one version and a version shifted by half a base-cell length. In many cases, the resulting microstructural topologies for two different base-cell geometries have an equal (and extremal) bulk modulus. Compared to the two-phase problems (Sigmund, 1999b) it seems that the three-phase problems have many more local minima and, therefore, the algorithm requires some more interaction by the user.

For further details on the inverse homogenization algorithm that we use and its application to various material design problems, the reader is referred to Sigmund (1994a, b, 1995, 1999a, b) and Sigmund and Torquato (1996, 1997).

3.2. Numerical results

In this section we demonstrate and discuss the results of the numerical optimization of two-dimensional three-phase composites. In all figures of this section the white regions are occupied by the weakest phase 1, the grey regions are filled by the intermediate phase 2, and the black regions correspond to the strongest phase 3. Note that the strongest phase is defined here as the phase with the highest value of the shear modulus. For each design, we show first, one periodic cell, and then a three by three array of these cells.

The base cell is discretized by 120×120 square finite elements with two design parameters (ρ_{23} and ρ_3) for each element; thus, there are 28,800 design variables. A finer discretization would result in a better description of the phase boundaries and a high value of the effective bulk modulus. However, this is not done due to restricted computational power.

For the first example, we design a composite made of three phases with the Young's moduli E_i, Poisson's ratios ν_i, and volume fractions f_i given by

$$E_1 = 0.0, \quad E_2 = 0.2, \quad E_3 = 1, \quad \nu_1 = \nu_2 = \nu_3 = 0.3, \quad f_1 = 0.2, \quad f_2 = 0.4, \quad f_3 = 0.4. \tag{28}$$

The bulk and shear moduli of each phase are then given by

$$\kappa_i = \frac{E_i}{2(1-\nu_i)}, \quad \mu_i = \frac{E_i}{2(1+\nu_i)}. \tag{29}$$

For these values of parameters the HSW upper bulk modulus bound $\kappa_U = 0.224$ is

greater than the phase 2 bulk modulus $\kappa_2 = 0.143$ and, therefore [see (15)], the bound is attainable by any of the schemes described in Section 2. The main goal of this example is to test the numerical algorithm and see whether it will be able to find the microstructure with bulk modulus close to the bound.

Two topology optimized microstructures are shown in Figs. 4 and 5. They both have effective bulk modulus $\kappa_* = 0.222$ which is within 1% of the theoretical bound. The difference is that the first structure has square symmetry of the effective tensor whereas the second one is isotropic. Computationally, it is easier to find a square symmetric structure. Therefore, for the other examples we will only consider square symmetric structures.

As expected, topologically the structures represent phase 1 and 2 inclusions in the matrix of phase 3. Phases 1 and 2 are never in contact with each other, they are always separated by phase 3. Fig. 4(c) shows a contour plot of the hydrostatic part of the strain fields for hydrostatic loading. It is close to being piece-wise constant, as it should be for the optimal structure.

The phases chosen for the second example have the same material properties

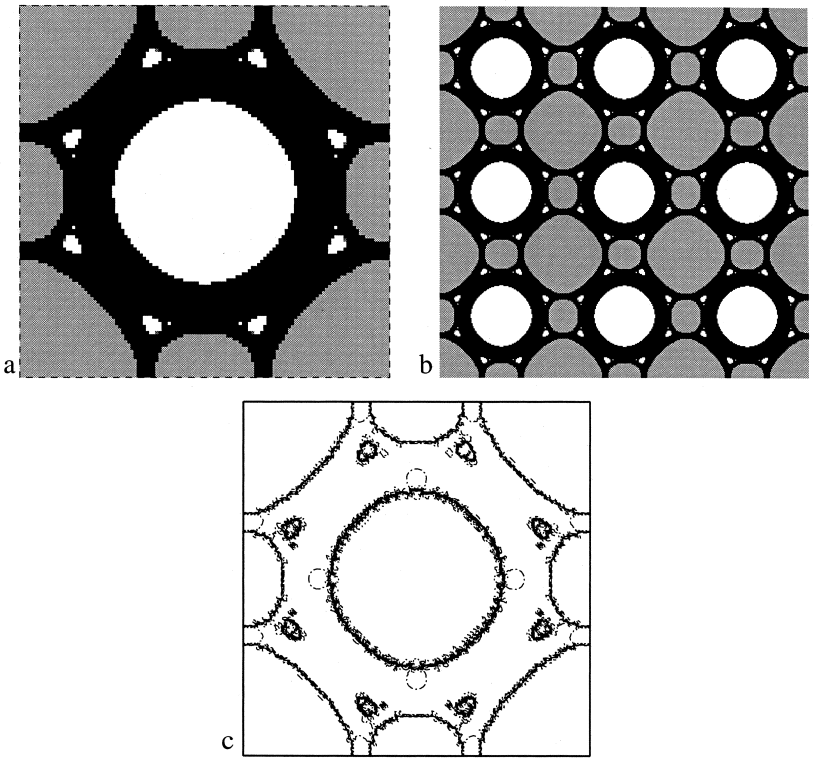

Fig. 4. Numerically obtained microstructure for parameters: $E_1 = 0$; $E_2 = 0.2$; $E_3 = 1$; $\nu_1 = \nu_2 = \nu_3 = 0.3$; $f_1 = 0.2$; $f_2 = 0.4$; and $f_3 = 0.4$. (a) One base cell, (b) three by three array of cells and (c) contour plot of the hydrostatic part $\varepsilon_{11} + \varepsilon_{22}$ of the local strain field $\varepsilon(x)$ for hydrostatic loading.

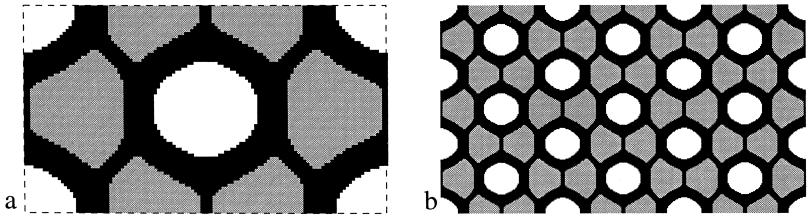

Fig. 5. Numerically obtained isotropic microstructure for parameters: $E_1=0$; $E_2=0.2$; $E_3=1$; $\nu_1=\nu_2=\nu_3=0.3$; $f_1=0.2$; $f_2=0.4$; and $f_3=0.4$. (a) One base cell, (b) three by three array of cells.

but taken in different volume fractions

$$E_1 = 0.0, \quad E_2 = 0.2, \quad E_3 = 1, \quad \nu_1 = \nu_2 = \nu_3 = 0.3, \quad f_1 = 0.5, \quad f_2 = 0.4, \quad f_3 = 0.1. \tag{30}$$

In this range of parameters the HSW bound $\kappa_U=0.0806$ cannot be achieved by previously known schemes, because $\kappa_U \leq \kappa_2=0.143$. The 'triple-coated microstructure' made of the space-filling arrangement of triple-coated circles of phases 1 in the core, 3 in the middle, and 2 in the outer coating, has the effective bulk modulus $\kappa_{231}=0.0729$. This value was suggested as a possible upper bound by Milton (1981). A similar conclusion follows from the optimal design scheme suggested by Lurie and Cherkaev (1984) for multiphase composites.

The topology optimized microstructure for this more challenging case is shown in Fig. 6 and has the effective bulk modulus $\kappa_*=0.0740$ numerically closer to the bound than κ_{231}. It clearly shows three different regimes: pure phase 1, pure phase 2, and a lamination of all three phases. The design is very similar to the microstructures shown in Sigmund (1999b) with an additional layer of phase 3 in

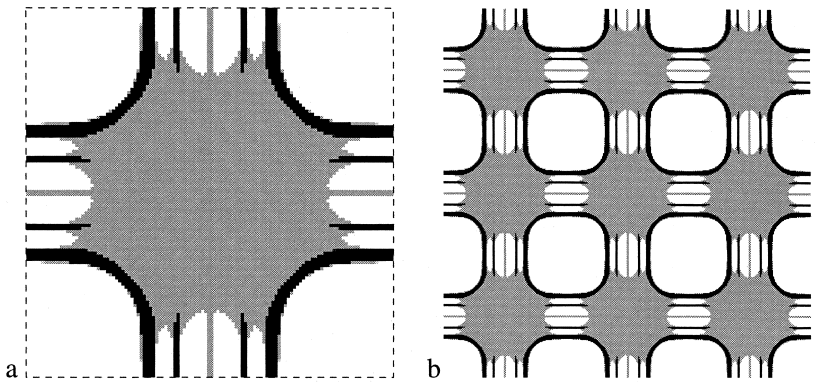

Fig. 6. Numerically obtained microstructure for parameters: $E_1=0$; $E_2=0.2$; $E_3=1$; $\nu_1=\nu_2=\nu_3=0.3$; $f_1=0.5$; $f_2=0.4$; and $f_3=0.1$. (a) One base cell, (b) three by three array of cells.

the laminate region. In the next section we will study the effective moduli of such a composite analytically.

The design shown in Fig. 7 is computed for the parameters

$$E_1 = 0.0, \quad E_2 = 0.3, \quad E_3 = 1, \quad \nu_1 = \nu_2 = \nu_3 = 0.3, \quad f_1 = 0.27, \quad f_2 = 0.7, \quad f_3 = 0.03. \tag{31}$$

Here, $\kappa_U = 0.142$ and $\kappa_{231} = 0.121$, and the effective bulk modulus of the optimized microstructure is equal to $\kappa_* = 0.115$. We observe the same characteristic features of the design. It consists of zones of pure phase 1 and pure phase 2, and zones occupied by a laminate composite of all three phases. The relatively high difference between the effective bulk modulus of this example and the bulk modulus $\kappa_{231} = 0.121$ can be explained by a low volume fraction of phase 3. This may require finer discretization to allow formation of laminate-type microstructure of phases 1 and 3.

For the next example we take

$$E_1 = 0.0, \quad E_2 = 0.2, \quad E_3 = 1, \quad \nu_1 = \nu_2 = \nu_3 = 0.3, \quad f_1 = 0.2, \quad f_2 = 0.7, \quad f_3 = 0.1. \tag{32}$$

Here we have

$$\kappa_U = 0.131, \quad \kappa_2 = 0.143, \quad \kappa_{231} = 0.130. \tag{33}$$

For this example, the HSW upper bound is not attainable by known designs. The topology optimized microstructure is shown in Fig. 8 and has effective bulk modulus $\kappa_* = 0.128$ which is within 3% of the bound. The structure has elements of the 'triple-coated circles' design. The central white circle with the ring of phase

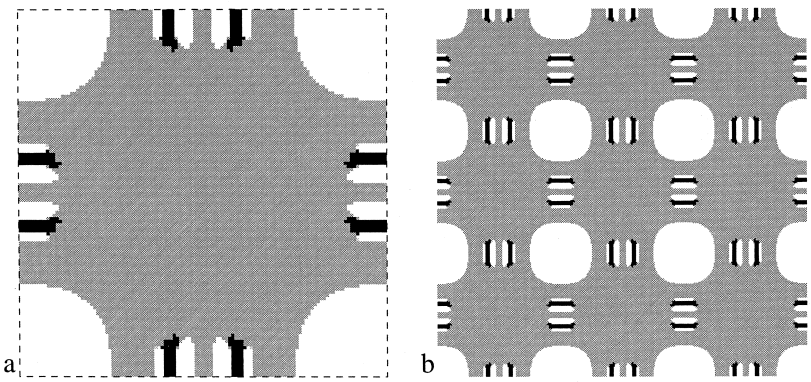

Fig. 7. Numerically obtained microstructure for parameters: $E_1 = 0$; $E_2 = 0.3$; $E_3 = 1$; $\nu_1 = \nu_2 = \nu_2 = 0.3$; $f_1 = 0.27$; $f_2 = 0.7$; and $f_3 = 0.03$. (a) One base cell, (b) three by three array of cells.

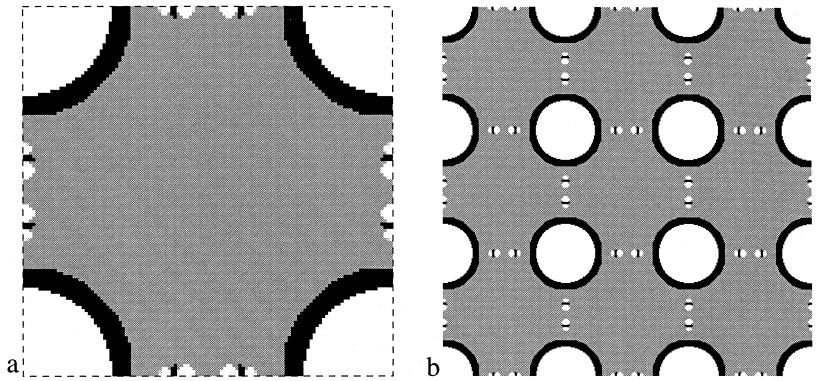

Fig. 8. Numerically obtained microstructure for parameters: $E_1=0$; $E_2=0.2$; $E_3=1$; $\nu_1=\nu_2=\nu_2=0.3$; $f_1=0.2$; $f_2=0.7$; and $f_3=0.1$. (a) One base cell, (b) three by three array of cells.

3 can be interpreted as a composite (of phase 1 and 3) with the effective bulk modulus κ_2. This composite is in turn surrounded by phase 2. Some amounts of phase 1 and 3 are used to make a laminated composite of these phases.

The last example has the following properties:

$$E_1 = 0, \quad E_2 = 1, \quad E_3 = 1, \quad \nu_1 = \nu_2 = -\nu_3 = 1/2, \\ f_1 = f_2 = f_3 = 1/3. \tag{34}$$

Here we have

$$\kappa_1 = \mu_1 = 0, \quad \kappa_3 = \mu_2 = 1/3, \quad \kappa_2 = \mu_3 = 1, \quad \kappa_{\mathrm{U}} = 1/3, \\ \kappa_{231} = 0.273. \tag{35}$$

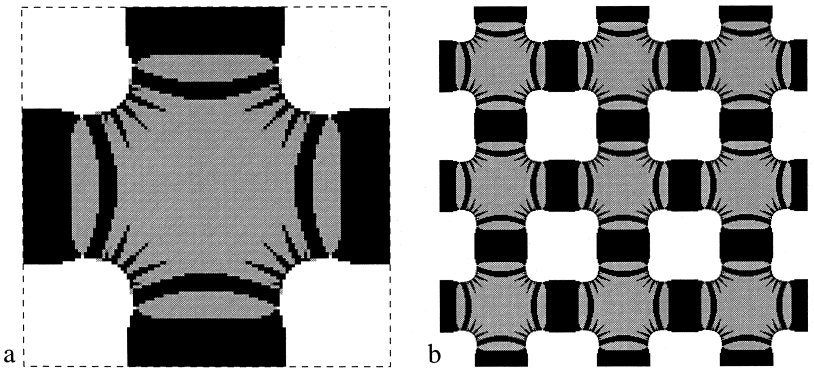

Fig. 9. Numerically obtained microstructure for parameters: $E_1=0$; $E_2=E_3=1$; $\nu_1=\nu_2=0.5$; $\nu_3=-0.5$; and $f_1=f_2=f_3=1/3$. (a) One base cell, (b) three by three array of cells.

These are 'non-well-ordered' phases: phase 3 which has the maximal shear modulus, has an intermediate bulk modulus. To the best of our knowledge, this case has not been studied in the literature. As it is easy to see, both analytical design schemes that were used to create a microstructure with an extremal bulk modulus fail in this situation. Indeed, the Milton (1981) design (see Fig. 2) cannot be implemented because the effective bulk modulus of any composites of phases 1 and 3 has a lower bulk modulus than any composite of phases 2 and 3. It is also impossible to implement the Lurie and Cherkaev (1984) design scheme because the effective bulk modulus of a composite of phases 1 and 3 is always smaller than κ_2. Numerically, we were able to find a design with the bulk modulus value $\kappa_* = 0.322$ for the microstructure shown in Fig. 9. This value is much higher than the value $\kappa_{231} = 0.273$ and within 4% of the HSW bound $\kappa_U = 1/3$.

As we see from the examples presented in this section, the numerically observed range of attainability of the HSW bounds is wider than it was previously believed. It seems that there are microstructures that possess bulk modulus close to the HSW bounds even for the small phase 3 volume fraction. Moreover, the topologies of the optimized microstructures provide some clues that will guide our analytical investigation. Our goal in the next section is to look for the analytical explanation of the numerical observations.

4. New structures

In this section we consider two-dimensional three-phase elastic composites. We first assume that

$$\kappa_1 \le \kappa_2 \le \kappa_3, \quad \mu_3 = \mu_{\max}. \tag{36}$$

Then the HSW bulk modulus upper bound (3) is given by

$$\kappa_U = \left[\frac{f_1}{\kappa_1 + \mu_3} + \frac{f_2}{\kappa_2 + \mu_3} + \frac{f_3}{\kappa_3 + \mu_3} \right]^{-1} - \mu_3. \tag{37}$$

One can check that the attainability condition $\kappa_U \ge \kappa_2$ is met if the volume fraction f_3 is sufficiently high, that is,

$$f_3 \ge f_3^*, \quad f_3^* = \frac{f_1(\kappa_3 + \mu_3)(\kappa_2 - \kappa_1)}{(\kappa_1 + \mu_3)(\kappa_3 - \kappa_2)}. \tag{38}$$

By using the relation $f_1 = 1 - f_2 - f_3$, condition (38) can also be presented in the form

$$f_3 \ge \hat{f}_3^*, \quad \hat{f}_3^* = \frac{(1 - f_2)(\kappa_3 + \mu_3)(\kappa_2 - \kappa_1)}{(\kappa_2 + \mu_3)(\kappa_3 - \kappa_1)}. \tag{39}$$

The microstructures that achieve the HSW upper bulk modulus bound for this range of parameters were described in Section 2.

In this section, we propose three new types (types I, II and III) of three-phase microstructures by combining the numerical observations of Section 3, field optimality conditions that require constant local fields in phases 1 and 2 of optimal composite, and the idea of Sigmund (1999b) for two-phase structures with an extremal bulk modulus.

4.1. Microstructure and effective bulk modulus of type I composites

Consider the microstructure with the unit square periodic cell shown schematically in Fig. 10. The corner $t \times t$ squares of the periodic cell are made of phase 2; the centre $(1-2t) \times (1-2t)$ square is occupied by phase 1; four $t \times (1-2t)$ rectangular domains are occupied by a laminate composite made of phases 1–3 taken in the volume fractions ρ_1, ρ_2, and ρ_3 ($\rho_1+\rho_2+\rho_3=1$), respectively. They are schematically shown by three strips of the phases 1–3. It is assumed here and throughout the paper that the length-scale of the lamination is much smaller than the size of the periodic cell so that the laminate composite can be treated as homogeneous anisotropic material illustrated in Fig. 10 by strips of different phases.

The total phase volume fractions are given and can be expressed via the geometrical parameters of the composite as

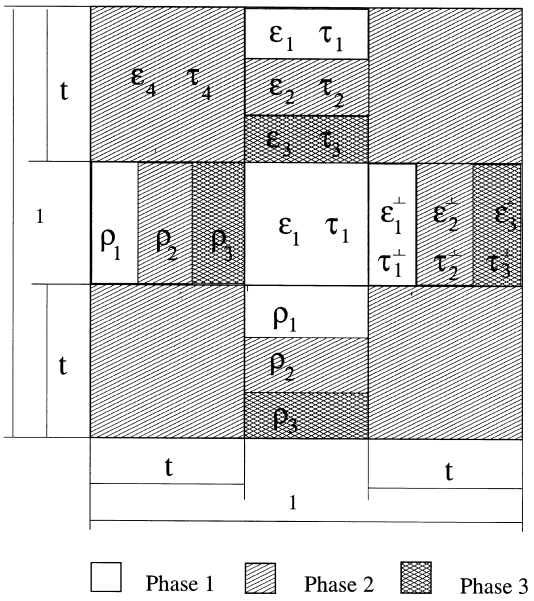

Fig. 10. Microstructure of type I composite. Local fields in phase 1 are constant for hydrostatic loading. Volume fraction of phase i in the laminate regions (schematically shown by three rectangulars of different phases) is given by ρ_i; ε_i and τ_i are the strain and stress fields in the corresponding regions, and $\varepsilon_i^{\perp}$ and $\tau_1^{\perp}$ are the fields rotated by $\pi/2$.

$$f_1 = (1-2t)^2 + 4t(1-2t)\rho_1,$$

$$f_2 = 4t^2 + 4t(1-2t)\rho_2, \tag{40}$$

$$f_3 = 1 - f_1 - f_2 = 4t(1-2t)\rho_3.$$

One can solve the system of Eqs. (40) to obtain the geometrical characteristics of the composite

$$\rho_1 = \frac{4t(1-t) - f_2 - f_3}{4t(1-2t)}, \quad \rho_2 = \frac{f_2 - 4t^2}{4t(1-2t)}, \quad \rho_3 = \frac{f_3}{4t(1-2t)} \tag{41}$$

as a function of phase volume fractions. Three geometrical parameters of the structure, that is, ρ_1, ρ_2, and t, allows one to find a suitable configuration for any phase volume fractions f_1, f_2, and f_3 provided the restriction

$$f_3 \le 2(\sqrt{f_2} - f_2) \tag{42}$$

holds. Indeed, as follows from (41),

$$\rho_1 \ge 0 \quad \text{if } t \in [(1-\sqrt{f_1})/2, (1+\sqrt{f_1})/2],$$

$$\rho_2 \ge 0 \quad \text{if } t \le \sqrt{f_2}/2,$$

$$\rho_3 \ge 0 \quad \text{if } t \le 1/2. \tag{43}$$

Thus, for any t in the interval

$$\frac{1-\sqrt{f_1}}{2} \le t \le \frac{\sqrt{f_2}}{2} \tag{44}$$

the system has a solution with parameters in the admissible region. The interval (44) is not empty if (42) holds.

Our next step is to find the effective bulk modulus of this composite. We will subject this composite to a hydrostatic average field and will look for the local strain fields $\varepsilon(x)$ and stress fields $\tau(x)$. Then the ratio of the hydrostatic parts of the average fields will define the effective bulk modulus.

We will look for the solution in the form

$$\varepsilon_1 = \begin{pmatrix} \varepsilon_1^h & 0 \\ 0 & \varepsilon_1^h \end{pmatrix}, \quad \varepsilon_2 = \begin{pmatrix} \varepsilon_2^h - \varepsilon_2^s & 0 \\ 0 & \varepsilon_2^h + \varepsilon_2^s \end{pmatrix},$$

$$\varepsilon_3 = \begin{pmatrix} \varepsilon_3^h - \varepsilon_3^s & 0 \\ 0 & \varepsilon_3^h + \varepsilon_3^s \end{pmatrix}, \quad \varepsilon_4 = \begin{pmatrix} \varepsilon_4^h & 0 \\ 0 & \varepsilon_4^h \end{pmatrix}, \tag{45}$$

where ε_1 is the constant strain field in phase 1, ε_4 is the strain field in the corner squares made of phase 2, ε_2 and ε_3 define the strain field in the laminate region of phases 2 and 3, respectively, as explained in Fig. 10. By symmetry, we expect the fields $\varepsilon_i^{\perp}$, $\tau_i^{\perp}$ in the vertical laminates to be a $\pi/2$ rotation of the fields in the horizontal laminates.

We require the phase 1 field to be constant because we expect the field in the weakest phase to be constant for the optimal composite. This assignment is the optimality requirement based on the field optimality conditions. The stress fields are defined by Hooke's law

$$\tau_1 = 2\begin{pmatrix} \kappa_1\varepsilon_1^h & 0 \\ 0 & \kappa_1\varepsilon_1^h \end{pmatrix}, \quad \tau_2 = 2\begin{pmatrix} \kappa_2\varepsilon_2^h - \mu_2\varepsilon_2^s & 0 \\ 0 & \kappa_2\varepsilon_2^h + \mu_2\varepsilon_2^s \end{pmatrix},$$

$$\tau_3 = 2\begin{pmatrix} \kappa_3\varepsilon_3^h - \mu_3\varepsilon_3^s & 0 \\ 0 & \kappa_3\varepsilon_3^h + \mu_3\varepsilon_{43}^s \end{pmatrix}, \quad \tau_4 = 2\begin{pmatrix} \kappa_2\varepsilon_4^h & 0 \\ 0 & \kappa_2\varepsilon_4^h \end{pmatrix}. \tag{46}$$

On phase boundaries, the fields should satisfy compatibility and equilibrium conditions

$$\varepsilon_1 = \varepsilon_2^h - \varepsilon_2^s = \varepsilon_3^h - \varepsilon_3^s,$$

$$\varepsilon_4^h = \rho_1\varepsilon_1 + \rho_2(\varepsilon_2^h + \varepsilon_2^s) + \rho_3(\varepsilon_3^h + \varepsilon_3^s),$$

$$\kappa_1\varepsilon_1 = \kappa_2\varepsilon_2^h + \mu_2\varepsilon_2^s = \kappa_3\varepsilon_3^h + \mu_3\varepsilon_3^s,$$

$$\kappa_2\varepsilon_4^h = \rho_1\kappa_1\varepsilon_1 + \rho_2(\kappa_2\varepsilon_2^h - \mu_2\varepsilon_2^s) + \rho_3(\kappa_3\varepsilon_3^h - \mu_3\varepsilon_3^s). \tag{47}$$

On the boundary of the laminate region these conditions are satisfied only 'on average'. We implicitly assume that the length scale of the lamination is much smaller than the size of the unit cell.

One can check (we did it by using the symbolic manipulation software Maple V) that the system (47) has a solution only for a special value of the parameter t given by

$$t = t_* = \frac{f_2}{2} + \frac{f_3}{2}\frac{(\kappa_2 + \mu_3)(\kappa_3 - \kappa_1)}{(\kappa_3 + \mu_3)(\kappa_2 - \kappa_1)}. \tag{48}$$

The right-hand-side inequality in (44) for the parameter $t = t_*$ is equivalent to the condition

$$f_3 \le f_3^{**}, \quad f_3^{**} = \frac{(\sqrt{f_2} - f_2)(\kappa_3 + \mu_3)(\kappa_2 - \kappa_1)}{(\kappa_2 + \mu_3)(\kappa_3 - \kappa_1)}, \tag{49}$$

where we always have $f_3^{**} \le \hat{f}_3^*$. As to the left-hand-side inequality in (44), it is

always satisfied. Indeed, for phase moduli ordered as specified by (36) the coefficient in front of $f_3/2$ in (48) achieves its minimum 1 if $\mu_3=0$ and $\kappa_1=0$. Therefore, t_* is always greater than $(f_2+f_3)/2$ and the difference

$$t_* - (1-\sqrt{f_1})/2 \geq (f_2+f_3)/2 - (1-\sqrt{f_1})/2 \geq (\sqrt{f_1}-f_1)/2 \geq 0 \tag{50}$$

is positive.

The effective bulk modulus of the microstructure is by definition equal to the ratio

$$\kappa_* = \frac{\langle \tau_{11}+\tau_{22}\rangle}{2\langle \varepsilon_{11}+\varepsilon_{22}\rangle}, \tag{51}$$

where

$$\langle \varepsilon_{11}+\varepsilon_{22}\rangle = 2(1-2t_*)^2\varepsilon_1^h + 8t_*(1-2t_*)(\rho_1\varepsilon_1^h + \rho_2\varepsilon_2^h + \rho_3\varepsilon_3^h) + 8t_*^2\varepsilon_4^h, \tag{52}$$

$$\begin{aligned}\langle \tau_{11}+\tau_{22}\rangle = {} & 4(1-2t_*)^2\kappa_1\varepsilon_1^h + 16t_*(1-2t_*)(\rho_1\kappa_1\varepsilon_1^h + \rho_2\kappa_2\varepsilon_2^h + \rho_3\kappa_3\varepsilon_3^h) \\ & + 16t_*^2\kappa_2\varepsilon_4^h\end{aligned} \tag{53}$$

are the average strain and stress fields. The shear parts of the local fields cancel out in (52) and (53) because the fields in the horizontal and vertical laminates differ by a rotation by $\pi/2$, or, equivalently, by the sign of the deviatoric part of the fields. However, dependence on phase shear moduli enters the ratio (51) via the solution of the system of equations that define local strains and stresses, and via the coefficient t_*.

The expression for the effective bulk modulus is rather long and will not be listed here. However, we have checked numerically that for sufficiently small phase 3 volume fraction [such that (49) holds] the composite that we just described has the largest value of the effective bulk modulus among all structures known to us if in addition to (36) the inequality

$$\mu_2 \geq \mu_1 \tag{54}$$

holds. Moreover, in this case it has correct asymptotic behaviour in the limit $f_3=0$ and degenerates into the optimal two-phase composite with the maximal bulk modulus found by Sigmund (1999b).

If the condition (49) holds as an equality, then the proportion ρ_2 of phase 2 in the laminate region hits zero, $\rho_2=0$. The proportions ρ_1 and ρ_3 of phases 1 and 3 at this point are equal to

$$\rho_1 = 1-\rho_3^*, \quad \rho_3 = \rho_3^*, \quad \rho_3^* = \frac{(\kappa_3+\mu_3)(\kappa_2-\kappa_1)}{2(\kappa_2+\mu_3)(\kappa_3-\kappa_1)}. \tag{55}$$

The local fields in phases 1 and 2 are constant and purely hydrostatic. But the most interesting fact is that the effective bulk modulus (51) is exactly equal to the

HSW bound! The calculation we did by using Maple V symbolic manipulation software. The result is rather unexpected: we found a microstructure that achieves the HSW bound at the point $f_3 = f_3^{**} < \hat{f}_3^*$ where the sufficient conditions (15) of attainability of the HSW bound are not met.

4.2. Microstructure and effective moduli of type II composites

If the volume fraction of phase 3 is larger than f_3^{**}, the value ρ_2 given by (41) becomes negative. Obviously, this is not admissible. But this is an indication of the direction of the process: the microstructure wants to move phase 2 from the laminate region to the corners. However, phase 2 in the laminates is already used. To circumvent the problem one can use a trick. Phase 2 can be 'imitated' as far as the bulk modulus is concerned, by the optimal mixture of phases 1 and 3 taken in the proportion

$$\gamma_* = \frac{f_3^*}{f_1} = \frac{(\kappa_2 + \mu_3)(\kappa_2 - \kappa_1)}{(\kappa_1 + \mu_3)(\kappa_3 - \kappa_2)}. \tag{56}$$

One can, therefore, make an isotropic mixture with the effective bulk modulus κ_2 by using some amount δ_1 of phase 1 and amount $\gamma_*\delta_1$ of phase 3. One then places the resulting material into the corners where it is mixed with phase 2 (see Fig. 11).

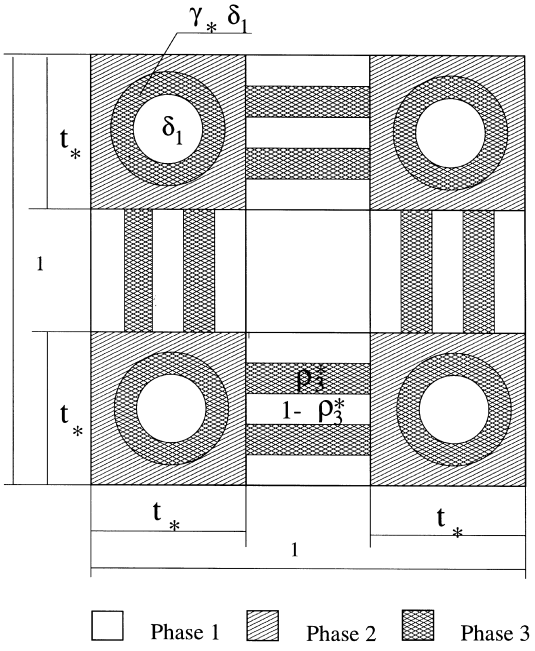

Fig. 11. Microstructure of type II composite with an effective bulk modulus equal to the HSW bound. Local fields in phases 1 and 2 are constant for hydrostatic loading.

Note that the goal is to prepare an optimal composite, and one would like to keep the proportion of phase 3 in the laminate region optimal, that is, given by ρ_3^*. The structure of the resulting composite is described by the conditions

$$f_1 - \delta_1 = (1-2t)^2 + 4(1-\rho_3^*)t(1-2t),$$

$$f_2 + \delta_1(1+\gamma_*) = 4t^2,$$

$$f_3 - \delta_1\gamma_* = 4\rho_3^* t(1-2t). \tag{57}$$

The system has two parameters, δ_1 and t, and two linearly independent equations

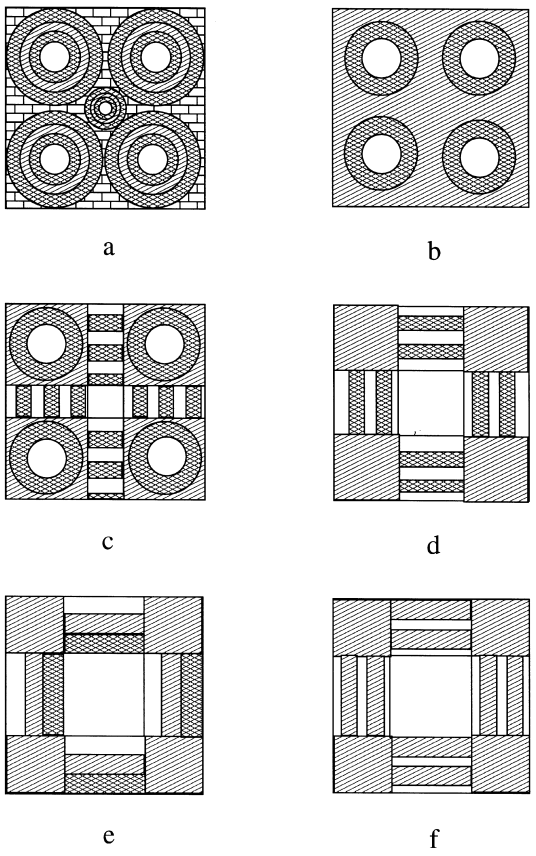

Fig. 12. Evolution of the microstructure: (a) optimal composite in the region where $\kappa_U \geq \kappa_2$; (b) optimal microstructure if $\kappa_U = \kappa_2$; (c) type II composite possesses bulk modulus $\kappa_* = \kappa_U \leq \kappa_2$ if $f_3 \in [f_3^{**}, f_3^*]$; (d) type II composite with $\kappa_* = \kappa_U \leq \kappa_2$ at the limit $f_3 = f_3^{**}$; (e) type I composite, with the bulk modulus $\kappa_* < \kappa_U$ higher than the one of any known structures if $f_3 < f_3^{**}$ and $\mu_2 > \mu_1$; (f) when phase 3 vanishes, the type I composite degenerates into the optimal two-phase structure.

with the third one being a linear combination of the other two. It has two solutions. The solution for the parameter t is exactly equal to plus or minus t_* where t_* is given by (48). One chooses the positive $t=t_*$. The solution for the parameter δ_1 is

$$\delta_1 = \frac{4t_*^2 - f_2}{1+\gamma_*}, \tag{58}$$

as can be found from the second equation in (57). It is positive if $4t_*^2 - f_2 \geq 0$, or equivalently, if $f_3 \geq f_3^{**}$. One can now check that there exists a piece-wise constant strain and stress field that delivers the solution to the system of compatibility equations of the type (47) (with $\rho_1 = 1-\rho_3^*$, $\rho_2 = 0$, and $\rho_3 = \rho_3^*$), and that the effective bulk modulus of the composite is equal to the HSW bound (37). Moreover, if $f_3 = \hat{f}_3^*$ then $\delta_1 = f_1$, $f_3 = \delta_1\gamma_*$, and $t_* = 1/2$. Thus, the type II composite is feasible and possesses an effective bulk modulus exactly equal to the HSW bound in the interval $f_3 \in [f_3^{**}, f_3^*]$.

4.3. Evolution of the microstructures

Our aim is to describe the evolution of the microstructural changes induced by the change in the initial parameters of the problem: phase moduli, and phase volume fractions. The process for the square symmetric composites is illustrated by Fig. 12. Note that the same procedure can be used to make an isotropic composite by using triangular or hexagonal topologies as was done by Sigmund (1999b) for two-phase structures. The stress and strain fields and the effective bulk modulus of triangular and hexagonal constructions are precisely the same (for the hydrostatic load) as in the square-based composites that we just described.

We start with the region of parameters where the HSW bound is known to be attainable, that is, when $\kappa_U \geq \kappa_2$. In this region, structures described in Section 2 provide the optimal solution. We chose to illustrate it by the triple-coated circles design (see Fig. 12(a)).

Then we move into the unknown region in the parameter space where the attainability conditions (15) are not satisfied, by either lowering the phase 3 volume fraction or by changing the parameter in some other way until the HSW bound (37) is exactly equal to κ_2. At this point, the external coating disappears from the coated circles, and possible realization of the microstructure with effective bulk modulus equal to κ_2 is the matrix of phase 2 material with circular inclusions of phase 1 surrounded by phase 3 to make them invisible (for the hydrostatic load) in the matrix of phase 2 (see Fig. 12(b)). The ratio of the volume fractions of phases 1 and 3 is exactly equal to γ_* given by (56).

If even less phase 3 material is available, the composite builds the type II microstructure shown in Fig. 12(c). The design of this composite is similar to Sigmund (1999b) structures. The central square is occupied by pure phase 1. Four corner squares are filled with the three-phase composite of pure phase 2, and phases 1 and 3 that are taken in the proportion γ_* defined by (56); the bulk

modulus of this composite is equal to κ_2. The corner squares are connected by the laminate composite of phases 1 and 3 taken in proportions $(1-\rho_3^*)$ and ρ_3^*, respectively. The microstructure of the composite is completely defined provided we know the phase volume fractions and the relative size of the corner squares taken as $t = t_*$.

When we further change the parameters of the problem, we always 'balance' it by moving phases 1 and 3 from the corner squares to the laminates. At some point we will use all the available amount of phases 1 and 3 in the corner squares (see Fig. 12(d)). At this point $f_3 = f_3^{**}$, the corner squares are made from pure phase 2. This is the boundary regime, that is, the last point in the parameter space when the composite has bulk modulus equal to the HSW bound. When we continue to change the parameters moving into the region where $f_3 \le f_3^{**}$, the type I microstructure (see Fig. 12(e)) becomes feasible and delivers the maximal bulk modulus. When phase 3 vanishes, the composite degenerates into the

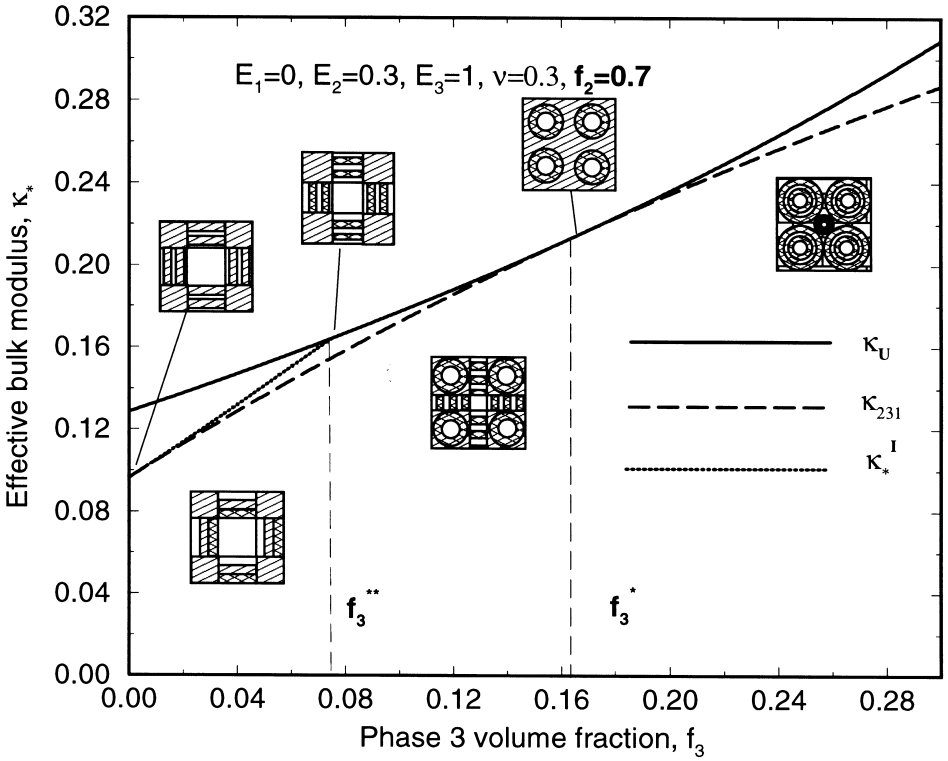

Fig. 13. Dependence of the effective bulk modulus on the phase 3 volume fraction. The solid line shows the HSW upper bound κ_U, the dashed line corresponds to the bulk moduli κ_{231} of the triple-coated circles, and the dotted line shows the values of the bulk moduli κ_*^I of the type I composite; type II composites attain the HSW bound if $f_3 \in [f_3^{**}, f_3^*]$. Small figures illustrate composite microstructures for each range of phase 3 volume fractions.

microstructure (see Fig. 12(f)) which is optimal for a two-phase design (Sigmund, 1999b). It has an effective bulk modulus exactly equal to the upper bound if the condition (54) holds.

The evolution of the effective bulk modulus with the change in the phase 3 volume fraction is shown in Fig. 13 for a composite made of three phases with the moduli and volume fractions given by

$$E_1 = 0, \quad E_2 = 0.3, \quad E_3 = 1, \quad \nu_1 = \nu_2 = \nu_3 = 0.3, \quad f_1 = 1 - f_2 - f_3, \\ f_2 = 0.7, \quad f_3 \in [0, 0.3]. \tag{59}$$

The solid line in Fig. 13 shows the HSW bulk modulus upper bound (37). The HSW bound was known to be attainable in the interval $f_3 \geq f_3^*$ where $\kappa_U \geq \kappa_2$. The dashed line shows the bulk modulus κ_{231} of the special type of composite made of the 'triple-coated' spheres (circles) with the core of phase 1, the intermediate ring of phase 3 and the external coating of phase 2. This is the value that was suggested by Milton (1981) as a possible upper bound for the effective bulk modulus in the region where $\kappa_U \leq \kappa_2$. The effective bulk modulus of the type II composite is exactly equal to the HSW bound in the interval $f_3 \in [f_3^*, f_3^{**}]$. The dotted line in the interval $f_3 \leq f_3^{**}$ corresponds to the effective bulk modulus of a type I composite. As we can see, the effective bulk modulus of this composite is larger than κ_{231}.

In our derivation we assumed that the phases satisfy the ordering condition (36). It is easy to see that the optimal microstructures and all the calculations for the type II composites which achieve the HSW bulk modulus upper bound in the interval $f_3 \in [f_3^{**}, f_3^*]$ are literally the same if we assume that

$$\kappa_3 \leq \kappa_2 \leq \kappa_1, \quad \mu_3 \geq \max\{\mu_1, \mu_2\}. \tag{60}$$

The only difference is that the attainability condition (15) is replaced by the inequality $\kappa_U \leq \kappa_2$. The calculation for the type I composite also does not change. It has the highest bulk modulus among all known structures if phase 2 has a higher shear modulus [see (54)].

4.4. Microstructure and effective moduli of type III composites

One difficulty associated with the design of multiphase elastic composites is that we have many phase parameters and, correspondingly, many design situations. In the previous sections we considered three-phase designs imposing ordering conditions (36) or (60) to prove optimality of our type II structures. We will not try to explore all the possible combinations of ordering, but consider one more example that corresponds to the 'non-well-ordered' phases of example 4, Section 3. Specifically, we assume that

$$\kappa_1 \leq \kappa_3 \leq \kappa_2, \quad \mu_3 = \mu_{\max}. \tag{61}$$

As we already mentioned, none of the previously known microstructures had an

effective modulus equal to the HSW bound in this range of the parameters. Here we suggest a new structure (type III composite) that possesses an extremal bulk modulus equal to the HSW bound.

The idea of the design is based on the field optimality conditions. Specifically, for the composite to attain the HSW upper bulk modulus bound the local fields in phases 1 and 2 must be hydrostatic and constant if the composite is subject to a hydrostatic average field. In types I and II microstructures subject to hydrostatic loading the local fields are hydrostatic and constant in the centre square and in the corner squares. By using this observation, we propose the following optimal design for the composite to achieve the HSW bound (see Fig. 14). In the centre square we place the weakest phase 1. In the corner squares we place the composite made of inclusions of phase 2 in the phase 3 matrix. The bulk modulus κ_{32} of this composite is defined by

$$\frac{1}{\kappa_{32}+\mu_3}=\frac{f_2/(f_2-\delta f_3)}{\kappa_2+\mu_3}+\frac{\delta f_3/(f_2+\delta f_3)}{\kappa_3+\mu_3}, \tag{62}$$

where δ is the portion of phase 3 used in the corner squares.

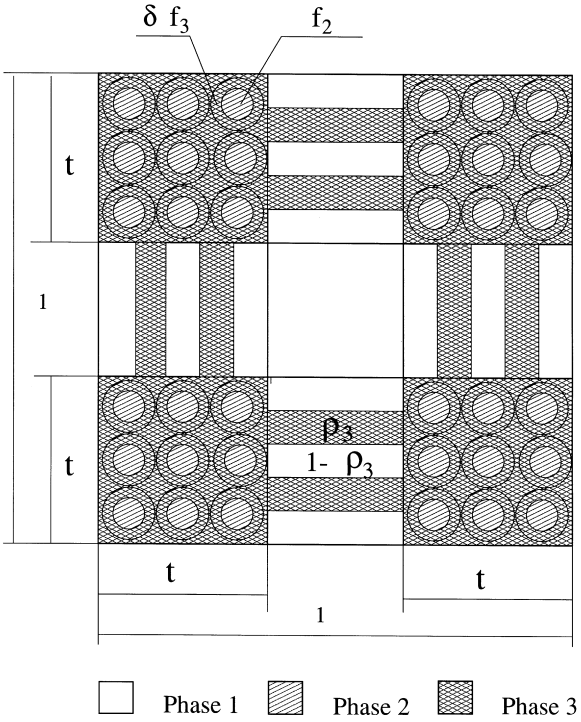

Fig. 14. Microstructure of type III composite with effective bulk modulus equal to the HSW bound. Local fields in phases 1 and 2 are constant for hydrostatic loading.

In the laminate region we place laminates of phase 1 and the remaining amount $(1-\delta)f_3$ of phase 3. The only free parameter δ of the microstructure defines the distribution of phase 3 between the corner squares and the laminate region. It should be chosen so that the field in phase 1 is hydrostatic and constant throughout the composite subject to hydrostatic loading.

The calculation is similar to the one that was needed to show optimality of the type II composite. We did it by using the Maple V program. The system of equations for the strain and stress fields has a solution if the parameter δ satisfies some quadratic equation. We were not able to find a sufficiently simple form of the solution to present it here but we have checked that the effective bulk modulus of the optimal structure is exactly equal to the HSW bound if the phase 3 volume fraction is higher than f_3^{**} given by (49).

Phase 3 vanishes from the corner squares when the optimal value δ_* of parameter δ is equal to zero, that is $\delta_*=0$. The microstructure degenerates to type

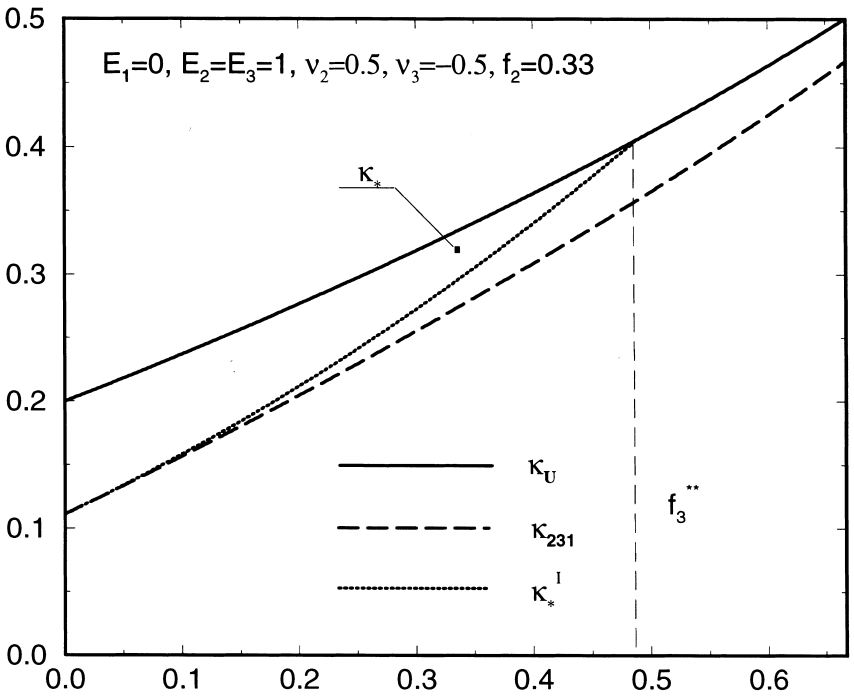

Fig. 15. Dependence of the effective bulk modulus on the phase 3 volume fraction. The solid line shows HSW upper bound κ_U, the dashed line corresponds to the bulk moduli κ_{231} of the triple-coated circles, and the dotted lines shows the values of the bulk moduli κ_*^I of the type I composite; type III composites attain the HSW bound if $f_3 \geq f_3^{**}$ topologically optimized structure (Fig. 9) possesses the bulk modulus κ_* shown by the small black box.

I design. Further evolution of the structure (when we decrease the phase 3 volume fraction) may follow the type 1 design. All the calculations of the previous section for the type I composite (with the three-phase laminate region) are literally the same. The type I microstructure may be feasible only if the phase 3 volume fraction is below the value f_3^{**} given by (49).

We would like to emphasize however, that the expressions for the geometrical parameters of type III composites are more complicated than the ones for type I and II structures. We were not able to verify whether the geometrical parameters of this composite (such as phase proportions in the laminations ρ_i and the δ-parameter) are within the obvious bounds $\rho_i \geq 0$, $i = 1, 2, 3$, $\delta_* \in [0, 1]$ for the general case or arbitrary phase moduli. We did it numerically for the particular example that is discussed below.

The evolution of the effective bulk modulus of the structures is shown in Fig. 15 for a composite made of three phases with Young's moduli E_i, Poisson's ratios ν, i and volume fractions f_i given by

$$\begin{aligned} &E_1 = 0, \quad E_2 = E_3 = 1, \quad \nu_1 = \nu_2 = 0.5, \quad \nu_3 = -0.5, \\ &f_1 = 1 - f_2 - f_3, \quad f_2 = 0.33, \quad f_3 \in [0, 0.67]. \end{aligned} \tag{63}$$

The solid line in Fig. 15 shows the HSW bulk modulus upper bound (37). The dashed line shows the bulk moduli κ_{231} of the 'triple-coated' circles with the core of phase 1, the intermediate ring of phase 3 and the external coating of the remaining phase 2. The dotted line in the interval $f_3 \leq f_3^{**}$ corresponds to the effective bulk modulus of type I composites. As we can see, the effective bulk moduli of these composites are larger than κ_{321}. The effective bulk modulus of the type III composite is exactly equal to the HSW bound in the interval $f_3 \geq f_3^{**}$.

As we already mentioned, the type III structures may not be the best for the combination of material properties discussed in this part. Indeed, numerically we were able to find a composite with a higher value of the effective bulk modulus. It is denoted as κ_* and is shown by the small black box in Fig. 15. The numerical design (see Fig. 9) indicates that the optimal composite should have regions of pure phase 1, and regions where phases 2 and 3 form a composite. However, we decided not to explore all the possible structures for all the possible combinations of parameters and leave it for future research.

5. Generalizations and summary of results

5.1. Interpretation of the numerical results

In this section we compare the results of the numerical optimization of Section 3 with the theoretical results of Section 4. For the first numerical example with the phase moduli and volume fractions given by (28) we have

$$f_1 = 0.2, \quad f_2 = 0.4, \quad f_3 = 0.4, \quad f_3^{**} = 0.097, \quad f_3^{*} = 0.143, \quad \hat{f}_3^{*} = 0.25. \tag{64}$$

As we can see, $f_3 \geq f_3^*$ and the bound $\kappa_U = 0.224$ is attainable by the Milton (1981) or Lurie and Cherkaev (1984) schemes. For this example, we found a new one-scale optimal structure shown in Figs. 4 and 5, with the effective bulk modulus $\kappa_* = 0.222$. It would be interesting to apply the Vigdergauz (1989, 1998) approach to find whether there exists an analytical solution for the shape of the optimal inclusions of phases 1 and 2 in the matrix of phase 3.

For the second example (30) we have

$$f_1 = 0.5, \quad f_2 = 0.4, \quad f_3 = 0.1, \quad f_3^{**} = 0.096, \quad f_3^{*} = 0.357, \quad \hat{f}_3^{*} = 0.25. \tag{65}$$

The HSW upper bound $\kappa_U = 0.0806$ is not attainable by the previously known schemes but attainable by the type II composite because $f_3 \geq f_3^{**}$. However, f_3 is very close to f_3^{**}. The type I and II structures coincide at the boundary value $f_3 = f_3^{**}$ and we may observe that the microstructure shown in Fig. 7 is almost of a type II topology. It has an effective bulk modulus $\kappa_* = 0.0740$.

For the design shown in Fig. 7 with the parameters (31) we have

$$f_1 = 0.27, \quad f_2 = 0.7, \quad f_3 = 0.03, \quad f_3^{**} = 0.075, \quad f_3^{*} = 0.33, \quad \hat{f}_3^{*} = 0.165. \tag{66}$$

The bound $\kappa_U = 0.142$ is not attainable by the type II composites because $f_3 \leq f_3^{**}$. We observe some characteristic features of type I composites: zones of pure phases 1 and 2, and the zone of the laminate composite of all three phases. The effective bulk modulus of the optimized microstructure is equal to $\kappa_* = 0.115$, the optimal type I composite has bulk modulus $\kappa_*^{\mathrm{I}} = 0.122$ higher than but close to $\kappa_{231} = 0.121$.

For example (32) we have

$$f_1 = 0.2, \quad f_2 = 0.7, \quad f_3 = 0.1, \quad f_3^{**} = 0.057, \quad f_3^{*} = 0.143, \quad \hat{f}_3^{*} = 0.125. \tag{67}$$

For these parameters, the HSW bound $\kappa_U = 0.131$ can be achieved by type II structures because $f_3 \geq f_3^{**}$. The topology optimized microstructure shown in Fig. 8 has the effective bulk modulus $\kappa_* = 0.128$ close to the HSW bound.

The parameters for the last example are defined by (34), and we have

$$f_1 = f_2 = f_3 = 1/3, \quad f_3^{**} = 0.488. \tag{68}$$

This is an example of a composite made of 'non-well-ordered' phases studied in

the last paragraph of Section 4. Specifically, phase 3 that has a maximal shear modulus has an intermediate bulk modulus. The type III composite cannot achieve the HSW bound $\kappa_U = 0.333$ for these parameters because $f_3 \le f_3^{**}$. The type I composite has a bulk modulus $\kappa_*^I = 0.294$ higher than the one given by the 'triple-coated' construction $\kappa_{231} = 0.273$. The microstructure shown in Fig. 9 has bulk modulus $\kappa_* = 0.322$.

5.2. Composites with minimal bulk modulus

In Sections 2–4 we considered the problem of maximization of the effective bulk modulus. The microstructure of two-dimensional composites with a minimal bulk modulus (or maximal effective compliance κ_*^{-1}) can be obtained by literally following the described procedure for composites with a maximal bulk modulus. The only difference is that the bulk and shear moduli κ and μ should be replaced by the bulk and shear compliances κ^{-1} and μ^{-1} in all the formulas of Sections 2–4 including conditions for the ordering of the phase moduli. Optimal composites of types 1 and II with a minimal bulk modulus can be obtained either by interchanging the positions of phases 1 and 3, or equivalently, by $\pi/2$ rotation of laminate directions in laminate composite zones.

One can then show that for well-ordered phases

$$\kappa_1 \le \kappa_2 \le \kappa_3, \quad \mu_1 \le \mu_2 \le \mu_3, \tag{69}$$

the HSW bulk modulus lower bound is attainable by type II composites (with interchanged positions of phases 1 and 3) if

$$\begin{aligned} &f_1 \in [f_1^{**}, \hat{f}_1^*], \quad f_1^{**} = \frac{(\sqrt{f_2} - f_2)(\mu_1 + \kappa_1)(\kappa_3 - \kappa_2)}{(\kappa_2 + \mu_1)(\kappa_3 - \kappa_1)}, \\ &\hat{f}_1^* = \frac{(1 - f_2)(\mu_1 + \kappa_1)(\kappa_3 - \kappa_2)}{(\kappa_2 + \mu_1)(\kappa_3 - \kappa_1)}. \end{aligned} \tag{70}$$

In the remaining range $f_1 \le f_1^{**}$ type I composites (with interchanged positions of phases 1 and 3) possess the smallest bulk moduli among all previously known composites with the same phase properties and volume fractions.

The same relation between the problems of maximization and minimization of the effective bulk modulus holds for the other cases of material ordering. Therefore, we only discuss composites with maximal bulk modulus, leaving the minimal bulk modulus problem as an obvious generalization.

5.3. Two-dimensional three-phase composites with extremal conductivity

Consider a two-dimensional composite of three conductors with the conductivity constants σ_1, σ_2, and σ_3, respectively, numbered so that

$$\sigma_1 \le \sigma_2 \le \sigma_3. \tag{71}$$

Milton (1981) and Lurie and Cherkaev (1984) have shown that the Hashin and Shtrikman (1962) conductivity upper bound

$$\sigma_* \le \sigma_U = \left[\frac{f_1}{\sigma_1+\sigma_2} + \frac{f_2}{\sigma_2+\sigma_3} + \frac{f_3}{\sigma_3+\sigma_3}\right]^{-1} - \sigma_3, \tag{72}$$

where σ_* is the effective conductivity of the composite, is attainable if $\sigma_U \ge \sigma_2$. One can check that this attainability condition is equivalent to the volume fraction restrictions

$$f_3 \ge f_3^{\#}, \quad f_3^{\#} = \frac{2f_1\sigma_3(\sigma_2-\sigma_1)}{(\sigma_1+\sigma_3)(\sigma_3-\sigma_2)} \tag{73}$$

or equivalently,

$$f_3 \ge \hat{f}_3^{\#}, \quad \hat{f}_3^{\#} = \frac{2(1-f_2)\sigma_3(\sigma_2-\sigma_1)}{(\sigma_2+\sigma_3)(\sigma_3-\sigma_1)}. \tag{74}$$

The results of Section 4 are readily applied to the two-dimensional three-phase conductivity problem. One can check that all the formulas of Section 4 are valid for conducting composites subject to the replacement

$$\kappa_i = \sigma_i, \quad \mu_i = \sigma_i, \quad \forall i. \tag{75}$$

Effective conductivities of type I and II composites are exactly equal to the effective bulk moduli of these composites made of phases with zero Poisson's ratio $\nu_i = (\kappa_i - \mu_i)/(\kappa_i + \mu_i)$ if (75) holds.

By using the type II composites described in Section 3 one can show that the HS bound is attainable if

$$f_3 \in [f_3^{\#\#}, f_3^{\#}], \quad f_3^{\#\#} = \frac{2(\sqrt{f_2}-f_2)\sigma_3(\sigma_2-\sigma_1)}{(\sigma_2+\sigma_3)(\sigma_3-\sigma_1)}, \tag{76}$$

where we always have $f_3^{\#} \le \hat{f}_3^{\#}$. In the remaining range of parameters, the composites of type I deliver effective conductivity that is higher than the effective conductivity of any previously known isotropic composite. However, optimality of these structures is not established. It would be interesting to check whether local fields in these composites satisfy the necessary conditions of optimality derived by Cherkaev (1999).

Similarly, for the problem of minimization of effective conductivity, we can use the formulas for the conductivity maximization problem with an obvious replacement of the conductivities σ_i by resistivities σ_i^{-1}. Below we summarize the result for conductivity minimization.

The HS lower bound on the effective conductivity

$$\sigma_* \ge \sigma_L = \left[\frac{f_1}{\sigma_1+\sigma_1} + \frac{f_2}{\sigma_2+\sigma_1} + \frac{f_3}{\sigma_3+\sigma_1}\right]^{-1} - \sigma_1, \tag{77}$$

was known to be attainable if $\sigma_L \leq \sigma_2$, or equivalently

$$f_1 \geq f_1^{@}, \quad f_1^{@} = \frac{2f_3\sigma_1(\sigma_3 - \sigma_2)}{(\sigma_1 + \sigma_3)(\sigma_2 - \sigma_1)}, \tag{78}$$

$$f_1 \geq \hat{f}_1^{@}, \quad \hat{f}_1^{@} = \frac{2(1 - f_2)\sigma_1(\sigma_3 - \sigma_2)}{(\sigma_1 + \sigma_2)(\sigma_3 - \sigma_1)}. \tag{79}$$

By using the composite of type II one can prove attainability of the HS lower bound in the interval

$$f_1 \in [f_1^{@@}, f_1^{@}], \quad f_1^{@@} = \frac{2(\sqrt{f_2} - f_2)\sigma_1(\sigma_3 - \sigma_2)}{(\sigma_1 + \sigma_2)(\sigma_3 - \sigma_1)}. \tag{80}$$

In the remaining range of the parameters $f_1 \leq f_1^{@@}$, type I composite with phase 3 in the centre square, is shown to have minimal effective conductivity constant among all known types of isotropic composites with given phase moduli and volume fractions.

Type II microstructures with maximal conductivity attain the HS bounds because the local fields in these composites are very special. In particular, the fields in phases 1 and 2 are constant. If the fields satisfy jump conditions on the phase boundaries in the square periodic cell (see Fig. 11), they will also be compatible if one resizes the microstructure, keeping the parameters γ_* and ρ_3^* fixed. The resulting microstructure is anisotropic and should exactly satisfy an anisotropic version of the HS bounds for two-dimensional three-phase composites (Zhikov, 1986; Kohn and Milton, 1988). This may lead to attainability requirements (for the anisotropic version of the HS bounds) that are less demanding compared with those derived for anisotropic multiphase composite by Kohn and Milton (1988).

Among other works on the effective properties of multiphase conductors we mention papers by Golden and Papanicolaou (1985), Golden (1986), Milton (1987a, b), Milton and Golden (1990), Nesi (1995), Cherkaev and Gibiansky (1996), Burns and Cherkaev (1997), and Cherkaev (1999). The list is by no means complete; one can find additional references in the aforementioned papers.

5.4. Summary of results and discussion

In Section 2, we listed the previously known results on the problem of maximization of the effective bulk modulus of multiphase linear elastic composites. Specifically, we presented the Hashin and Shtrikman (1963) and Walpole (1966) bounds on the effective bulk modulus, and two schemes (Milton, 1981; Lurie and Cherkaev, 1984) that allow one to build a composite with effective bulk or shear modulus exactly equal to the bulk or shear modulus

bound provided some restrictions on phase properties and volume fractions hold.

In Section 3, we applied a topology optimization procedure (Sigmund, 1994a, b, 1995, 1999a; Sigmund and Torquato, 1996, 1997) to look for two-dimensional three-phase composites with a maximal effective bulk modulus. We found composites with an effective bulk modulus close to the HSW bound even when the sufficient conditions of attainability (listed in Section 2) were not satisfied. The microstructures of the optimized composites were topologically similar to the ones observed by Sigmund (1999b) for optimal two-phase composites. They clearly demonstrated regions where the phases formed a laminate composite. The numerical procedure delivered microstructures with bulk moduli that are within a few percent of the theoretical bounds.

Based on these results and field optimality conditions necessary for the attainability of the HSW bounds, we found a new type of optimal composite that achieves the HSW upper bulk modulus bound in a range of parameters where the bound cannot be obtained by previously known schemes. The most complete results were obtained for well-ordered phases (69). We demonstrated that the upper bulk modulus bounds can be obtained by a special type of composite (type II, Section 4) if the stiff phase 3 volume fraction f_3 lies in the interval

$$f_3 = [f_3^{**}, f_3^{*}], \quad f_3^{*} = \frac{(1-f_2)(\kappa_3+\mu_3)(\kappa_2-\kappa_1)}{(\kappa_2+\mu_3)(\kappa_3-\kappa_1)},$$
$$f_3^{**} = \frac{(\sqrt{f_2}-f_2)(\kappa_3+\mu_3)(\kappa_2-\kappa_1)}{(\kappa_2+\mu_3)(\kappa_3-\kappa_1)}. \tag{81}$$

These structures allow one to achieve the HSW bulk modulus bound in the interval where it was not possible by using previously known composites. Thus, we show that the interval of attainability of the HSW bulk modulus bounds is much wider than was previously believed. Moreover, our new attainability condition $f_3 \geq f_3^{**}$ is more natural than $f_3 \geq f_3^{*}$ in a sense that it allows for a smooth transition to the two-phase design when the volume fraction of phase 2 is equal to zero. The condition $f_3 \geq f_3^{*}$ at this limit requires the phase 3 volume fraction to be sufficiently large. As we know, for two-phase composites the HSW bulk modulus bounds are always attainable.

In the remaining interval $f_3 \leq f_3^{**}$ the HSW bound cannot be achieved by the proposed structures due to geometrical restrictions. However, another type of composite (type I, Section 4) possesses bulk moduli higher than the bulk moduli of any previously known composite with the same phase properties and volume fractions. The type I and II structures coincide at the boundary value $f_3 = f_3^{**}$.

For the case of phase ordering conditions similar to (61) we have found new type III composites that may exactly satisfy the HSW modulus bound if the phase 3 volume fraction is sufficiently high, $f_3 \geq f_3^{**}$.

For two phases, the results can be extended to three dimensions (Sigmund, 1999b). In this case, the optimal microstructures consist of convex disjoint polygonal regions of pure soft or stiff phase connected by laminated plates and transversely isotropic rods made from mixtures of the two material phases. Most probably, some of the three phase results presented in this paper can be extended to the three dimensional case, however this exercise is left for future studies.

This study demonstrated that a combination of analytical and numerical methods of studying inverse homogenization problems allows for the effective use of the best features of both approaches. It would be interesting to apply this dual approach to study multiphase composites with an extremal shear modulus and corresponding three-dimensional problems.

Acknowledgements

L.G. gratefully acknowledges the support by the DCAMM International Graduate Research School and the Danish Research Academy, and the hospitality of the Danish Center for Applied Mathematics and Mechanics. O.S. gratefully acknowledges the support by the Danish Technical Research Council [THOR/ Talent-programme: Design of MicroElectroMechanical Systems (MEMS)].

References

Bendsøe, M.P., 1995. Optimization of Structural Topology, Shape and Material. Springer, New York.

Bendsøe, M.P., Kikuchi, N., 1988. Generating optimal topologies in optimal design using a homogenization method. Comp. Meth. Appl. Mech. Engng 71, 197–224.

Bensoussan, A., Lions, J.L., Papanicolaou, G., 1978. Asymptotic Analyses of Periodic Structures. North-Holland, Amsterdam.

Burns, T., Cherkaev, A.V., 1997. Optimal distribution of multimaterial composites for torsional beams. Struct. Opt. 13 (1), 1–4.

Bourgat, J.F., 1977. Numerical experiments of the homogenization method for operators with periodic coefficients. In: Lecture Notes in Mathematics, vol. 704. Springer-Verlag, Berlin, pp. 330–356.

Cherkaev, A.V., 1999. Necessary conditions technique in structural optimization. Int. J. Solids Struct., in press.

Cherkaev, A.V., Gibiansky, L.V., 1996. Extremal structures of multiphase heat conducting composites. Int. J. Solids Struct. 33 (18), 2609–2623.

Francfort, G., Murat, F., 1986. Homogenization and optimal bounds in linear elasticity. Arch. Rational Mech. Anal. 94, 307–334.

Golden, K., 1986. Bounds on the complex permittivity of a multicomponent material. J. Mech. Phys. Solids 34 (4), 333–358.

Golden, K., Papanicolaou, G., 1985. Bounds for effective parameters of multicomponent media by analytic continuation. J. Stat. Phys. 40, 655–667.

Grabovsky, Y., Kohn, R.V., 1995. Microstructures minimizing the energy of a two phase elastic composite in two space dimensions. II: the Vigdergauz microstructure. J. Mech. Phys. Solids 43 (6), 949–972.

Guedes, J.M., Kikuchi, N., 1991. Preprocessing and postprocessing for materials based on the homogenization method with adaptive finite element methods. Comp. Meth. Appl. Mech. Eng. 83, 143–198.

Hashin, Z., 1965. On elastic behaviour of fibre reinforced materials of arbitrary transverse phase geometry. J. Mech. Phys. Solids 13, 119–134.

Hashin, Z., Shtrikman, S., 1962. A variational approach to the theory of the effective magnetic permeability of multiphase materials. J. Appl. Phys. 35, 3125–3131.

Hashin, Z., Shtrikman, S., 1963. A variational approach to the theory of the elastic behaviour of multiphase materials. J. Mech. Phys. Solids 11, 127–140.

Jikov, V.V., Kozlov, S.M., Oleinik, O.A., 1994. Homogenization of Differential Operators and Integral Functionals. Springer, New York.

Kohn, R.V., Milton, G.W., 1988. Variational bounds on the effective moduli of anisotropic composites. J. Mech. Phys. Solids 36 (6), 597–629.

Lurie, K.A., Cherkaev, A.V., 1984. The problem of formation of optimal isotropic multiphase composite. Preprint 895, Ioffe Physico-Technical Institute, Leningrad. Shorter version in J. Opt. Th. Appl. 46, 571–589, 1985.

Milton, G.W., 1981. Concerning bounds on the transport and mechanical properties of multicomponent composite materials. Appl. Phys. A 26, 125–130.

Milton, G.W., 1986. Modeling the properties of composites by laminates. In: Ericksen, J.L., Kinderlehrer, D., Kohn, R., Lions, J-L. (Eds.), Homogenization and Effective Moduli of Materials and Media. Springer-Verlag, New York, pp. 150–174.

Milton, G.W., 1987a. Multicomponent composites, impedance networks and new types of continued fraction I, II. Commun. Math. Phys. 111, 281–327.

Milton, G.W., 1987b. Multicomponent composites, impedance networks and new types of continued fraction I, II. Commun. Math. Phys. 111, 329–372.

Milton, G.W., Golden, K., 1990. Representation for the conductivity functions of multicomponent composites. Comm. Pure Appl. Math. 18, 647–671.

Nesi, V., 1995. Bounds on the effective conductivity of 2-D composites made of $n \geq 3$ isotropic phases in prescribed volume fraction: the weighted translation method. Proc. Roy. Soc. Edinburgh A 125 (6), 1219–1239.

Norris, A.N., 1985. A differential scheme for the effective moduli of composites. Mech. Mat. 4, 1–16.

Sanchez-Palencia, E., 1980. Nonhomogeneous Media and Vibration Theory. Lecture Notes in Physics, Springer, Berlin, p. 127.

Sigmund, O., 1994a. Materials with prescribed constitutive parameters: an inverse homogenization problem. Int. J. Solids Struct. 31 (17), 2313–2329.

Sigmund, O., 1994b. Design of material structures using topology optimization. Ph.D. thesis, Department of Solid Mechanics, Technical University of Denmark. DCAMM special Report No. 69.

Sigmund, O., 1995. Tailoring materials with prescribed elastic properties. Mech. Mat. 20, 351–368.

Sigmund, O., 1997. On the design of compliant mechanisms using topology optimization. Mech. Struct. Mach. 25 (4), 495–526.

Sigmund, O., 1999a. On the optimality of bone microstructure. In: Pedersen, P., Bendsøe, M.P. (Eds.), Synthesis in Bio Solid Mechanics. Kluwer, pp. 221–234 Proceedings of IUTAM, May 1998.

Sigmund, O., 1999b. A new class of extremal composites. J. Mech. Phys. Solids, 48(2), 397–428.

Sigmund, O., Petersson, J., 1998. Numerical instabilities in topology optimization: a survey on procedures dealing with checkerboards, mesh-dependencies and local minima. Struct. Opt. 16 (1), 68–75.

Sigmund, O., Torquato, S., 1996. Composites with extremal thermal expansion coefficients. Appl. Phys. Lett. 69 (21), 3203–3205.

Sigmund, O., Torquato, S., 1997. Design of materials with extreme thermal expansion using a three-phase topology optimization method. J. Mech. Phys. Solids 45 (6), 1037–1067.

Vigdergauz, S.B., 1989. Regular structures with extremal elastic properties. J. Mech. Phys. Solids 24 (3), 57–63.

Vigdergauz, S.B., 1994. Three-dimensional grained composites of extreme thermal properties. J. Mech. Phys. Solids 42 (5), 729–740.

Vigdergauz, S.B., 1999. Energy-minimizing inclusions in a planar elastic structure with macroisotropy. Struct. Opt., 17(2–3), 104–112.

Walpole, L., 1966. On bounds for the overall elastic moduli of inhomogeneous systems I. J. Mech. Phys. Solids 14, 151–162.
Zhikov, V., 1986. On the estimates for the trace of homogenized matrix. Math. Notes 40, 628–634.